Geomorphology 462 (2024) 109324

Contents lists available at ScienceDirect

Geomorphology

journal homepage: www.journals.elsevier.com/geomorphology

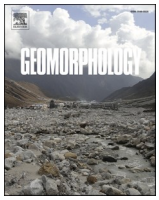

# Observed beach nourishment development in a semi-enclosed coastal embayment

Anna Adell [a,b,*], Aart Kroon [b], Björn Almström [a], Magnus Larson [a], Caroline Hallin [a]

[a] Division of Water Resources Engineering, Lund University, Box 118, SE-221 00 Lund, Sweden
[b] Department of Geosciences and Natural Resource Management, University of Copenhagen, Øster Voldgade 10, 1350 Copenhagen, Denmark

ARTICLE INFO

*Keywords:*
Coastal embayment
Beach nourishment
Coastal erosion
Storm response
Sediment transport
Coastal management

ABSTRACT

Beaches are important coastal features that provide vital ecosystem services; however, these systems are threatened by coastal erosion, sea-level rise, and coastal squeeze. Beach nourishments are a commonly applied coastal protection measure to mitigate erosion and flood risks while maintaining or enhancing recreational values. Nourishments vary in scale from mega-nourishments to small-scale nourishments, where the latter has typically been less studied due to the limited resources for monitoring. Meanwhile, with rising sea levels, the implementation of small-scale nourishments is expected to increase, and there is a need for more knowledge about the morphological evolution and technical lifetime of these interventions. In this study, the morphological responses of small-scale beach nourishment (total volume 20,000 $m^3$ which amounts to 30 $m^3$ added per m alongshore) are observed and quantified over various timescales, considering the initial adjustment, long-term development, and event-driven response. The investigated nourishment is implemented in a partly sheltered coastal embayment in the semi-enclosed Baltic Sea, which has a complex interaction between waves and water levels. Furthermore, the beach is surrounded by hard structures, a rock revetment at the back, and a harbor mole and a groin, influencing the longshore and cross-shore sediment transport. The results show that substantial reduction in subaerial volume can be attributed to specific events. In addition, we observed considerable spatial variation in the sediment re-distribution induced by hard structures and variability in the nearshore bathymetry. The lifetime of the beach nourishment is just over two years. The nourished material remains in the system at the end of the lifetime but is not available for beach recovery. Still, the added subaerial volume has eroded at the midsection, and the protective beach width has been reduced, leaving the rock revetment exposed with reduced protection for the hinterland. The energy conditions at the site are highly episodic, which impacts morphological evolution, and observations indicate that the development is event-driven.

## 1. Introduction

Beaches are important coastal features that offer erosion and flood protection for the hinterland, provide vital ecosystem services, and have recreational value. Their ability to dissipate wave energy and reduce wave runup can protect low-lying areas from flooding, makes beaches a natural defense against coastal hazards (Barbier et al., 2011; Defeo et al., 2009). The morphology of beaches is influenced by hydrodynamic forcing, and the variation in the magnitude of forcing drives to natural variability in the beach morphology (Davidson-Arnott, 2010; Nielsen, 2009). Due to climate change, projections show that there will be an increase in hydrodynamic impact for coastal areas, globally through sea level rise and locally through increased frequency and intensity of storms (Beniston et al., 2007; Oppenheimer et al., 2019; Vousdoukas et al., 2017). These changes in forcing due to climate change will influence long-term coastal evolution, meaning that previously stable or accreting beaches may start to erode (Luijendijk et al., 2018; Vousdoukas et al., 2020). To be able to keep relying on and benefit from the services inhabited by beach environments, there is a need for efficient coastal management and planning strategies.

In areas where landward retreat of sandy beaches is not desired, sand nourishments are commonly applied as a coastal protection strategy to mitigate erosion and flood risks (De Schipper et al., 2021; Hanson et al., 2002; Van Rijn, 2011). In addition to coastal protection, sand nourishment can provide alternative functions, such as recreation, beneficial use of dredged sediment volumes (Spodar et al., 2018), and have

* Corresponding author at: Division of Water Resources Engineering, Lund University, Box 118, SE-221 00 Lund, Sweden.
*E-mail address:* anna.adell@tvrl.lth.se (A. Adell).

https://doi.org/10.1016/j.geomorph.2024.109324
Received 27 March 2024; Received in revised form 19 June 2024; Accepted 25 June 2024
Available online 27 June 2024

environmental benefits (De Schipper et al., 2021). The strategy implies altering the sediment budget by artificially placing sediment within the morphologically active coastal zone, i.e., from the depth of closure to the dune (Dean, 2002).

The size of the nourishment depends on the dynamics of the environment in which they are implemented and the type of nourishment, e.g., beach fill, shoreface, channel wall, or mega nourishment (Brand et al., 2022; Van Rijn, 2011). For design purposes, it is important to understand the site-specific dynamics for morphological development. For instance, open coastlines lining the world's oceans are exposed to a range of wind waves, storm surges, and tides. These environments are highly dynamic, and beach morphology presents distinct seasonal and intra-annual variability due to the variations in forcing (e.g., Vos et al., 2023). In contrast, beaches in sheltered coastal environments and embayments are typically characterized by the forcing of low to moderate wave conditions (Jackson et al., 2002). The wave activity in low-energy, semi-enclosed basins is highly episodic and alternates between high-energy events created under strong wind conditions followed by calm periods with weak winds (Jackson et al., 2002). This means that storms are dictating the morphology of low-energy beaches, and the possibility of recovery under less energetic conditions may be limited (Gallop et al., 2020; Jackson et al., 2002). The event-driven morphology for these systems impacts the sediment transport rates, which are typically lower than for open coasts. Moreover, the active coastal zone is smaller, leading to smaller nourishment projects.

Large-scale nourishments (>100 $m^3$ per m alongshore) have been extensively implemented and studied across the globe (e.g., Brand et al., 2022; Dean, 2002; Hanson et al., 2002; Pilkey et al., 1989). The lifetime is typically 1–5 years, depending on the type of nourishment and coastal type, and often, regular maintenance is required to maintain the beach width (Van Rijn, 2011). In recent decades, mega nourishments (>500 $m^3$ per m alongshore) have received extensive attention and research funding, e.g., the *Sand Engine* (De Schipper et al., 2016; Stive et al., 2013) and the *Hondsbossche Dunes* project (Kroon et al., 2022) in the Netherlands. Mega-nourishments significantly alter the coast and are typically designed to last and supply the adjacent coastline with sediment for decades. In contrast, small-volume nourishment projects (<100 $m^3$ per m alongshore) have received less attention. Small-volume projects are common in an urban setting and are often implemented in combination with hard structures. Due to their limited extent and budgets, this often implies limited resources for monitoring activities and evaluation of the effectiveness of the protection.

Nourishment projects with smaller volumes have been applied and studied in sheltered coastal environments, such as estuaries (Andrade et al., 2006; Jackson and Nordstrom, 1994; Lowe and Kennedy, 2016), lakes (O'Brien et al., 1999; Ton et al., 2021), or inland seas (Basterretxea et al., 2007; Corradi et al., 2008; Karasu et al., 2023; Ojeda and Guillén, 2008; Pupienis et al., 2014). However, the hydrodynamic and morphological settings of the studied systems vary greatly, making it challenging to generalize design guidelines. Furthermore, it is difficult to evaluate the success of small-volume nourishment interventions, especially in environments with episodic wave activity. Longer datasets are needed to evaluate the performance of nourishments in low-energy systems where storms control the morphology. Thus, there is limited understanding of how persistent the added sediment volumes are in the low-energy systems, and very few studies evaluate the lifetime of the protection.

Since the number of small-scale projects is expected to increase with rising sea levels and spread to areas with no previous experience, more knowledge is needed on the behavior of small-scale nourishments in sheltered environments. Nourishing with smaller volumes can be beneficial because it reduces the impact on marine environments compared to larger operations (Corradi et al., 2008). In addition, small-volume nourishment projects can be a good option to utilize dredged sand volumes from navigation channels or harbors and can be a cost-effective alternative (Muñoz-Perez et al., 2001). Furthermore, small-scale nourishments can be implemented in combination with hard structures, e.g., as reinforcement to increase the safety levels (Blott and Pye, 2004) or mitigate their adverse effects on sediment dynamics.

The present study aims to understand and quantify the morphological responses of a nourished beach in a sheltered coastal embayment with episodic wave activity and basin effects influencing hydrodynamic conditions. The analysis is based on three years of field data and observations. The primary objective is to evaluate the effectiveness of the small-scale nourishment by quantifying morphological evolution like subaerial volume changes and alterations in shoreline position. It considers three types of responses: the initial adjustment of the nourishment, the long-term change over a couple of years, and the storm response to an event with extreme waves and water levels. Additionally, we identify the main drivers for morphological development and estimate the lifetime defined as the time it takes for the added volume to distribute from its original position in a way that the protective capabilities of the nourishment protection are compromised.

## 2. Regional setting and study site description

The study site in Faxe Ladeplads, Denmark, is located in the Arkona Basin in the Baltic Sea, a semi-enclosed sea in northern Europe, extending over latitudes 54-66° N and longitudes 10-30° E (Fig. 1). Water exchange between the North Atlantic and the Baltic Sea is limited through the shallow Danish straits. Since the basin covers a relatively large area (392,978 $km^2$), there is a great spatial variation in the characteristics of the sub-basins and physical and environmental conditions (Leppäranta and Myrberg, 2009). The Arkona Basin is one of the shallowest parts of the Baltic Sea, with a mean depth of 23 m and a maximum depth of 53 m.

The tidal range in the Baltic Sea is very small (<10 cm) and can often be considered neglectable. However, water level variations occur due to several other processes. During long periods with strong westerly and north-westerly winds, the inflow to the Baltic Sea can be substantially larger than normal and can increase the average sea level by up to 0.5 m for the entire basin (Hünicke et al., 2015). Shorter-term water level fluctuations arise from storm surges, e.g., wind-driven setup and atmospheric pressure variations (Weisse et al., 2021). In addition, the water level can fluctuate due to an inherent basin oscillation, i.e., seiches. Seiches are observed oscillations in partly enclosed water bodies (e.g., harbors and lakes), but the phenomenon also influences sea level dynamics on larger scales in semi-enclosed seas, like the Baltic Sea, where they happen in relation to wind variations (Hellström, 1941; Metzner et al., 2000).

In the Arkona Basin, westerly directions dominate most annual wave fields. The intra-annual variability in magnitude and direction of annual wave energy flux shows a clear positive correlation to the North Atlantic Oscillation (NAO) (Adell et al., 2023). Variations in wind direction characterized by the NAO also influence the sea level variations in the Baltic Sea basin (e.g., Johansson et al., 2001; Omstedt et al., 2004; Suursaar et al., 2006; Woolf et al., 2003). The confined nature of the Baltic Sea makes basin effects that impact water level variations, such that the water level is highly influenced by wind setup and set down. For the Arkona basin, westerly winds give lower water levels as water masses are being pushed towards the east part of the Baltic Sea. This water mass returns to the western part of the Baltic Sea if the wind ceases, which means that water level variations are alternating in relation to the wind direction with a varying time delay (Bendixen et al., 2013). High water levels mainly arise from eastern winds pushing water from the east Baltic to the Arkona Basin. There are a few known occasions where the returning water masses from the east were strengthened by wind setup from easterly storms. The most well-known example is the catastrophic flooding event in 1872 that killed nearly 300 people in the region (Hallin et al., 2021).

The coasts in the Arkona Basin mainly consist of Quaternary soft sediments, and their morphology is dictated by permanent transgression

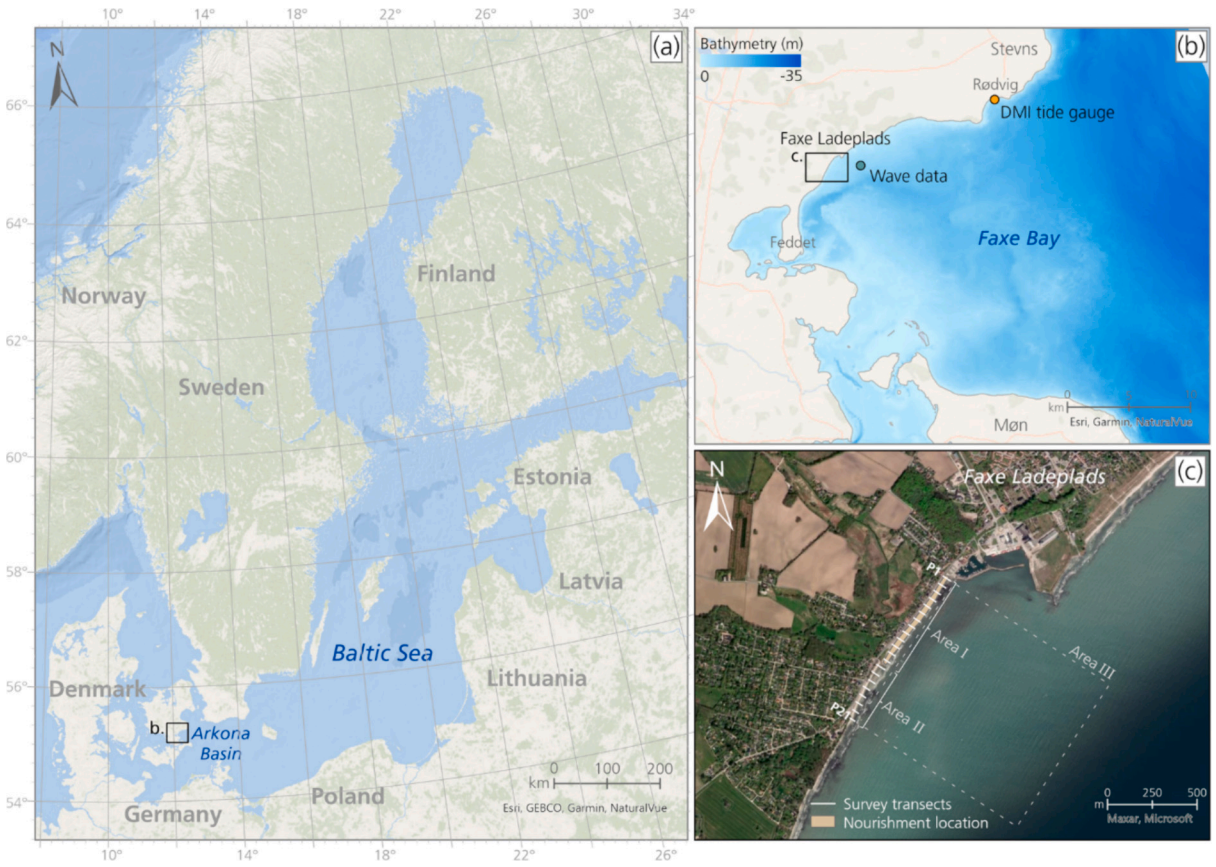


**Fig. 1.** (a) Map over the Baltic Sea indicating the location of the study site, (b) Map over Faxe Bay with bathymetry data of 50 × 50 m resolution provided by (Masetti et al., 2022), (c) The study site at Faxe Ladeplads and the extent of field survey campaigns, with 21 survey transects labeled P1–21. The nourishment covers Area I, i.e., transects P1–13, and Area II, transects P14–21, represents the downdrift area.

(Harff et al., 2017). This region is subsiding as the post-glacial uplift is limited. Currents induced by gradients in water levels are weak, and waves are the dominant energy component to drive nearshore sediment transport processes and govern beach morphology (Dissanayake et al., 2023; Eelsalu et al., 2022). The morphological response of embayed Baltic Sea beaches is a product of a few annual events that represent a significant part of the total incoming wave energy flux (Eelsalu et al., 2022). The most significant changes to the coasts occur when large waves and high water levels coincide, bringing the highest risk of coastal flooding and erosion (Bendixen et al., 2013; Hanson and Larson, 2008; Orvikut et al., 2003), which is expected to increase with rising sea levels.

The study site is in Faxe Bay (Fig. 1b), a shallow embayment with a mean depth of <15 m. The bay is confined between the two headlands, Stevns Klint to the north and Møns Klint to the south, which are limestone cliffs. The coastline in the bay is dominated by narrow sand-gravel beaches and eroding coastal cliffs composed of sedimentary glacial deposits (Luetzenburg et al., 2023), along with harbors and infrastructure located in the coastal zone. The littoral drift is directed from the northeast to the south in the bay. At the end of the littoral system is the accretive feature Feddet peninsula, a sandy spit where longshore transported sediment is deposited in ridges (Bendixen et al., 2013).

The beach at Faxe Ladeplads is sheltered from the predominant wind direction, which is west-southwest. The energy conditions for the region are defined by storms of high intensity and typically short duration, alternating with prolonged periods of low wave energy (Aagaard, 1990). The largest and most frequent waves approach the beach from the southeast direction (wave rose Fig. 2c), where the largest fetches are between 230 and 310 km. In the other directions, wave growth is limited by the short fetches, and significant wave heights are typically <1 m.

The harbor of Faxe Ladeplads (Fig. 1c), which serves shipping and leisure sailing, disrupts the sediment influx to the beach from the northeast. There is a reoccurring problem with material deposition in the navigation channel, which is dredged several times yearly and deposited offshore. Over time, the protruding harbor has caused advancement of the coastline updrift (by 60–100 m in 70 years, visible from aerial photos), while the downdrift areas have suffered chronic erosion due to the lack of sediment input.

Historically, the erosion downdrift has been mitigated with a groin field between the harbor mole and the terminal groin. About two decades ago, the groins were removed as they were severely worn down and no longer had an effect. Only the terminal groin remains, with a concrete wall and rock revetment to protect houses and infrastructure (Fig. 2). Just south of the groin a small creek discharge into the bay, with a river discharge < 1 $m^3/s$. The crest height of the concrete wall measures +3.5 m at maximum, and the elevation of the road behind is about +3.0 m. In November 2018 and July 2021, small-scale nourishments (70,000 $m^3$ and 20,000 $m^3$, respectively) were installed in front of the revetment to reduce overtopping during extreme storm events and restore the beach for recreation. The sediment was placed in Area I, i.e., transects P1-P13 (Fig. 1c).

Following the 2018 nourishment, there was a relatively quick redistribution of sediment in the cross-shore direction; sediment was transported from the subaerial part of the beach to the subaqueous. This was due to the long-term coastal erosion that had caused sediment loss of the profile. The profile adjustment was driven by three storm events that occurred in the 2018 winter period, shortly after the nourishment was completed. The cross-shore energy components were higher than the longshore components, causing this cross-shore material redistribution and the profile adjustment towards equilibrium (Danish Coastal Authority, 2021). The reduction of beach width at the nourished


**Fig. 2.** Overview of the managed coastal stretch. (a) Schematic cross-section of the protection; heights are indicated in m DVR90. (b) Drone image from July 2021, just after completing the nourishment, Photo: Danish Coastal Authority. (c) Satellite image (Google Earth Pro version 7.3.6, image date: 2019/08/25) with important attributes indicated.

site after the first winter period with storms led to a second nourishment in 2021, which is the focus of this study. The sediment was placed in exactly the same location as the 2018 nourishment.

## 3. Datasets and methods

### 3.1. Hydrodynamic data

Hourly water level data is available from the Danish Meteorological Institute (DMI) tide gauge at Rødvig Harbor, located 14 km northeast of the study site (Fig. 1b). Levels are referred to mean sea level in DVR90 (Danish Vertical Reference in 1990). The water level data used in the analysis were extracted from 2012/01/01 to 2023/12/31. A quality control, including comparison to nearby gauge records, was conducted to discard anomalies. The mean water level over the period 2012–2023 was 0.12 m above the reference level.

Hourly wave data for the same period was simulated in SWAN (Booij et al., 1999) with a regional hindcast wave model (Adell et al., 2023).

The same model set-up and calibration configuration were used as described in Adell et al., (2023), which has been validated for offshore and nearshore performance. Data used in the continued analysis was extracted at 7 m depth, outside the breaking zone, at the site of the location, see Fig. 1b. The significant wave heights ($H_s$) were transformed to root-mean-square wave height ($H_{rms}$) by the relationship $H_{rms} = H_s/1.416$. This was then used to compute the daily and monthly wave energy densities during the study period, by summing hourly wave energy for each day and month respectively.

### 3.2. Morphological data

Topographic and bathymetric field surveys were conducted at the site in Faxe Ladeplads from June 2021 to November 2023 (Table 1). The survey area covered the nourished beach section with a longshore distance of 630 m (Area I) and an additional 350 m downdrift (Area II) (Fig. 1c). Topographic and bathymetric surveys were conducted with RTK-GNSS to measure the subaerial beach and shallow nearshore area, extending approximately 70 m seaward from the toe of the revetment. Transects collected with the RTK-GNSS (cm accuracy) were placed with an alongshore spatial distance of 50 m. A total of 21 transects were placed along the 1 km stretch. The local reference system UTM zone 32N is used for the positional data, and elevation data is given in DVR90. The pre-nourishment condition is represented by a survey conducted in a campaign on 2020/06/09 by the Danish Coastal Authority (2021). Nearshore data (Area III) was measured using a zodiac research vessel with a single beam echosounder and sonar. The soundings were filtered for waves simply by using a spline function. The vertical accuracy was in the order of 0.1 m, which is large compared to the bed level changes and could therefore not be used to estimate volume changes but only to estimate the position of depth contours.

The data measured with RTK-GNSS is used to compute the subaerial beach volume for each survey transect over time. The landward boundary to compute the volume under the profile is defined at the toe of the rock revetment, and the seaward boundary is located at the shoreline, which is defined as the most landward intersection with $z = 0$ m DVR90. Furthermore, to estimate the total subaerial volume, the volume under each transect is multiplied by 50 m, according to the assumption that each transects is representative for a section of 50 m longshore.

When a berm is present in the profile, the subaerial beach is divided into an upper beach and a beach face. The slope of the upper beach is defined between the landward boundary and the berm crest, while the slope of the beach face is defined as the slope between the berm crest and the 0-m contour. If no berm is present, the elevation at the landward boundary is used.

## 4. Results

### 4.1. Hydrodynamic conditions under the survey period

Fig. 3 presents a scatter plot of the joint occurrence of water levels and significant wave heights during the survey period. The hydrodynamic conditions are classified into four groups. The significant wave heights were divided into two groups, to distinguish the storm wave heights using the threshold of the 95$^{th}$ percentile $H_s$. The mean water level over the study period was used to divide all water level data. Four quadrants appeared, and the percentage of occurrence showed a clear distinction. In 51.2 % of the cases, we observed relatively high water levels with low to moderate wave conditions. The most energetic conditions with high waves and water levels only occurred in 4 % of the observations. This distinction in occurrence also becomes apparent when looking at the distributions presented by the histograms alongside the scatter plot. The faded colors in the histograms correspond to the entire available dataset (2012/01/01–2023/12/31), and the dark colors correspond to the survey period (2021/06/01–2023/12/31).

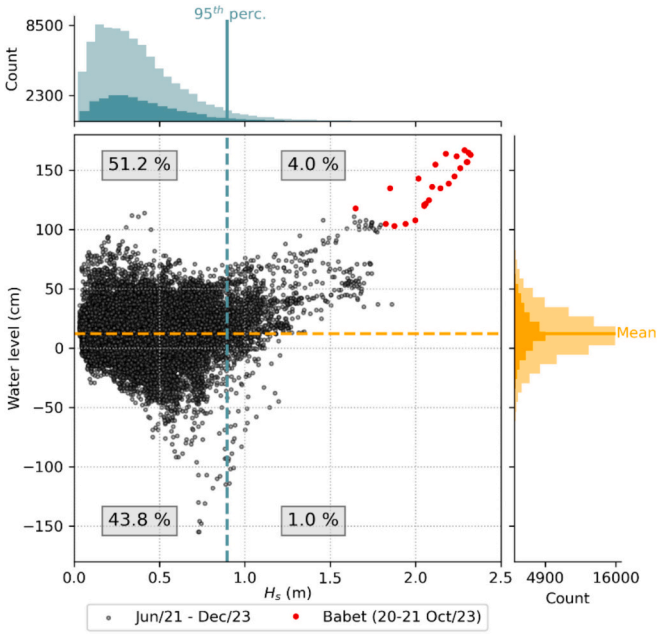


**Fig. 3.** Hydrodynamic conditions during the survey period based on water level data from the DMI tide gauge at Rødvig (available open-access https://www.dmi.dk/friedata/observationer/) and simulated waves. Levels of the extreme storm surge of October 2023 (Babet) are indicated in red. Threshold lines correspond to long-term (based on data from 2012 to 2023) mean water level, 12 cm (orange), and long-term 95$^{th}$ percentile significant wave height, 0.9 m (turquoise).

Fig. 4 summarizes the wave conditions in the area from June 2020 to December 2023. The sum of the monthly wave energy density is presented along with the number of hours that the wave height is above the threshold (95$^{th}$ percentile $H_s$) each month. Babet contributed to making October 2023 the month with the highest wave energy, followed by December 2022. The first year after the nourishment was introduced, July 2021–June 2022, was a relatively calm year regarding wave action. Only December 2021 and March 2022 indicate the occurrence of some higher duration where $H_s$ exceeded the 95$^{th}$ percentile. The next period, July 2022–June 2023, had more high energy events with notably varying distribution over the seasons. This means that the recovery times between events were shorter.

The survey period is deemed to represent a characteristic period when compared to the long-term dataset, apart from the 20–21 October 2023 storm surge Babet, indicated by the red dots in Fig. 3. The conditions during storm Babet correspond to both the highest waves and highest water levels during the survey period as well as in the entire available dataset. Before storm Babet, water levels in the Baltic Sea basin were already elevated by 40 cm above normal due to a period dominated by westerly winds earlier in October that had pushed water from the North Sea to the Baltic Sea (Swedish Meteorological and Hydrological Institute, 2023). Two days before the storm, the wind direction shifted

**Table 1**
Information about the dates for the conducted field surveys each year.

| Year | Area | Dates (month/day) |
|---|---|---|
| 2020 | Beach (I, II) | 06/09* |
| 2021 | Beach (I, II) | 09/03, 10/04*, 12/10 |
| | Nearshore (III) | 05/11, 06/15, 09/03, 10/04, 12/14 |
| 2022 | Beach (I, II) | 01/18, 02/24, 05/18 |
| | Nearshore (III) | 01/18, 03/02, 06/21 |
| 2023 | Beach (I, II) | 06/15, 10/18, 10/23, 11/10 |
| | Nearshore (III) | 11/10 |

* Data provided by the Danish Coastal Authority.

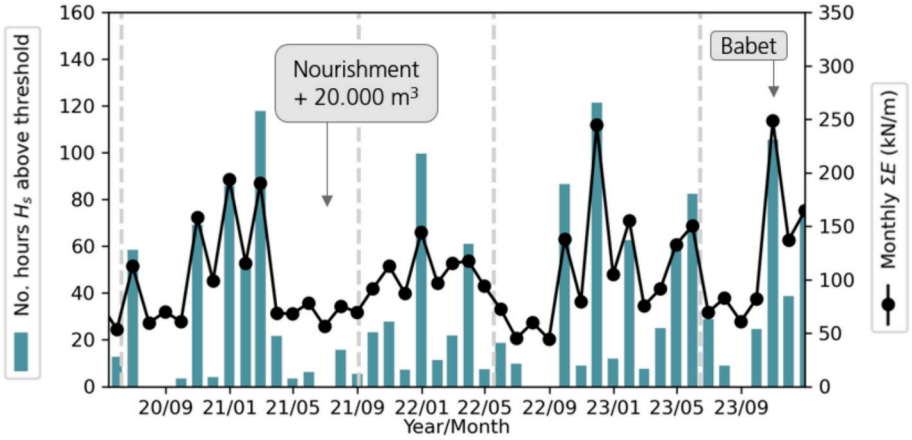


**Fig. 4.** The sum of monthly wave energy (black line) and the number of hours each month that $H_s$ is above the threshold 95$^{th}$ percentile $H_s$ = 0.9 m (bars). The dashed grey lines indicate the time for annual profile surveys.

from west to east and increased in intensity. The storm peak was reached the night between October 20$^{th}$ and 21$^{st}$. The strong easterly winds (25 m/s mean wind speed and 30 m/s gust wind speed, according to Swedish Meteorological and Hydrological Institute, 2023) drove substantial wind setup at the southwestern part of the Baltic Sea and simultaneously generated large waves. At the peak of the storm, water levels reached 169 cm DVR90 and waves were approaching from the southeast with a maximum simulated significant wave heights of 2.3 m at the study site (Fig. 5).

### 4.2. Morphological change

#### 4.2.1. Initial adjustments after the nourishment

The initial profile adjustment after the nourishment is illustrated by transect P9 (Fig. 6) since this profile is placed in the most dynamic and central part of the nourished area. In Fig. 6a, the black dotted line represents the pre-nourishment conditions from the 2020/06/09 survey; then the subaerial part of the beach is narrow, 7.7 m, and the beach face slope is steep, 0.18. The aqua green line represents the conditions on 2021/09/03, shortly after the completion of the nourishment. Then, the subaerial part of the beach has extended to a width of 32.8 m, giving a wide upper beach with a mild slope of 0.022 and a beach face slope of 0.15.

The development in the following six months is illustrated as bed level difference between consecutive observations together with the wave and water level conditions between observations (Fig. 6b-e). In addition, Fig. 7 shows the time series of daily total wave energy density during the first six months of the survey period to better illustrate the wave forcing conditions preceding the observations, which are marked with vertical dashed lines and the diamonds represent the available nourishment volume in transect P9.

The 2021/2022 winter had low exceedance of the storm wave height threshold defined as the 95$^{th}$ percentile $H_s$ (Fig. 4). The yellow line in Fig. 6a represents the observation from 2021/12/10, just after a high-energy wave event. Compared to the previous observation, the beach has eroded. The panel showing the elevation change indicates a reduction of beach elevation of >0.5 m, and erosion occurs over almost the entire extent of the cross-shore profile, from 8 to 42 m cross-shore distance (Fig. 6a). The shoreline position, defined at 0 m DVR90, retreaded by 5 m, and the subaerial volume in the transect decreased by 11.8 m$^3$/m between 2021/10/04 and 2021/12/10 (Fig. 7). The scatter plot in Fig. 6c (right panel) also shows that this period was the only period since introducing the nourishment that experienced both high waves and high water levels simultaneously for an extended duration. This explains why the erosion was observed across the whole cross-shore profile. The maximum $H_s$ was 1.53 m from the southeast and coincided with water levels of 80 cm DVR90 during the event.

The third period, 2021/12/10 to 2022/01/18, (Fig. 6d) was dominated by relatively mild conditions with only a small increase in incoming wave energy on December 27–28, corresponding to a

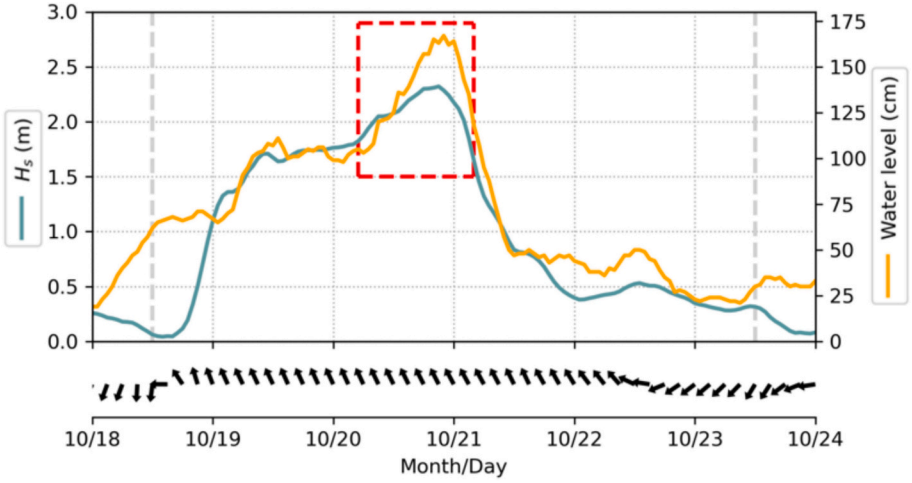


**Fig. 5.** Timeseries of waves and water level during storm Babet. The arrows below indicate the wave direction, and the red box corresponds to the levels under the storm peak that are indicated with red dots in the scatter plot in Fig. 3. Dashed grey lines mark the time for pre- and post-storm of profile observations.

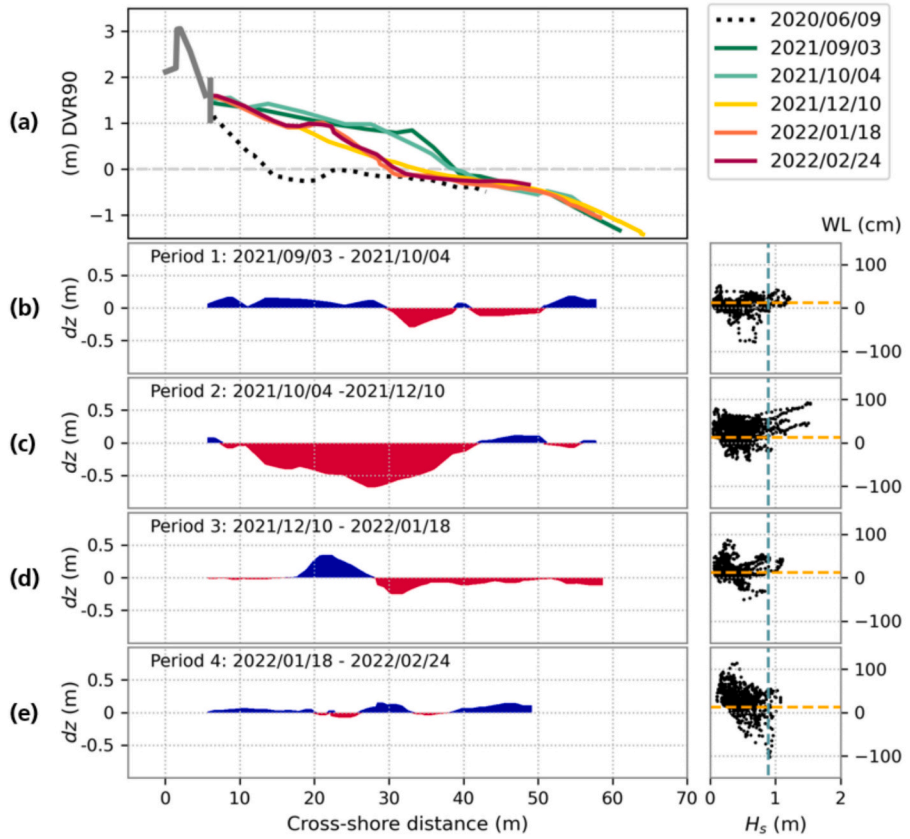


**Fig. 6.** Initial profile adjustment (5 months) for transect P9 located in the center section of the nourished stretch. Panel (a) shows the profile configuration over time, and panels (b-e) show the elevation difference between two consecutive surveys, where red indicates erosion and blue indicates deposition. Scatter plots to the right show the hydrodynamic conditions between two consecutive survey dates.

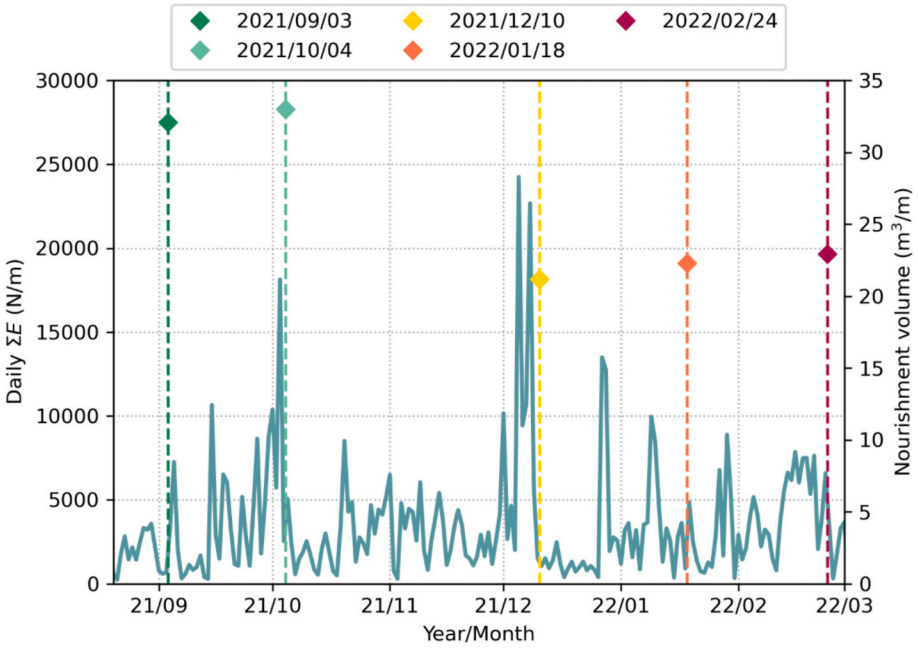


**Fig. 7.** Daily wave energy during the first months of the survey period, 2021/09–2022/03. The dashed lines mark the time of the profile observations, and the diamonds correspond to the available volume in the transect P9 displayed in Fig. 6.

maximum $H_s$ of 1.10 m and water level of only +40 cm DVR90. The cross-shore profile change indicates the formation of a beach berm and a steepening of the beach face slope from 0.06 to 0.11. The following fourth period, 2022/01/18 to 2022/02/24 (Fig. 6e), was also characterized by mild conditions, which induced minimal changes observed in the profile; the berm and beach face slope are stable in this period.

During the initial adjustment, the first six months of the survey period, about 20 % of the added nourishment volume is eroded from the subaerial beach. This substantial volume change can be attributed to the high energy event on 5–8 December 2021, and during the following calmer periods, only slight adjustments through the development of morphological features, such as formation of a berm is observed. During the same period, the area downdrift from the nourishment is relatively stable, and only very limited changes are observed. These include intermittent formation and erosion of the slip-face of the swash bar at shallow water depth; morphological features are present although not particularly pronounced.

#### 4.2.2. *Long-term changes over a period of three years*

The intra-annual volume change of the subaerial part of the profiles is presented in Fig. 8. Volume changes between surveys and for the entire extent of the investigated coastline cover three years of morphological change in the study area. Surveys from the same season are used for the comparison, i.e., 2020/06/09, 2021/09/03, 2022/05/18, and 2023/06/15.

The nourishment is placed between the harbor mole and the groin with the purpose of forming an alongshore uniform beach with a width of 40 m. However, the pre-nourishment conditions of the beach and nearshore showed a longshore variability of the shoreline position with a narrower beach in the middle and a wider beach adjacent to the structures. Before the nourishment, there was no material in the subaerial part of the profiles for transects P7–10, and the rock revetment was exposed. Fig. 8a shows the observed volume change between 2020 and 2021. There is an increase in subaerial beach volume after the nourishment and larger sediment volumes were added to the mid-section of the beach to create a longshore uniform beach width.

In the following two years, sediment from the subaerial beach is eroded in transect P2-P12 (Fig. 8b and c). The total volume eroded from the subaerial beach corresponds to 2620 $m^3$ for September 2021 – May 2022 and 4629 $m^3$ for June 2022 – June 2023. The increase in volume change documented for the second period can be explained by the relatively calm wave conditions July 2021 – June 2022 (Fig. 4). Furthermore, the May 2022 survey followed a month with very mild conditions, while the June 2023 survey followed a relatively stormy period where $H_s$ over 0.9 m for 60 h in May 2023 and 80 h in June 2023, respectively. A positive volume change in the subaerial beach was primarily observed in transects P1 and P13, i.e., near the harbor mole and groin, respectively.

The total change since the nourishment until June 2023 (Fig. 8d) shows that the added volume has eroded from the subaerial beach in the central part and that the cross-shore transect P8 is back to a state corresponding to the initial condition before the nourishment. All panels in Fig. 8 shows a distinct spatial variability in the volume change, indicating that the presences of hard structures influence the morphological

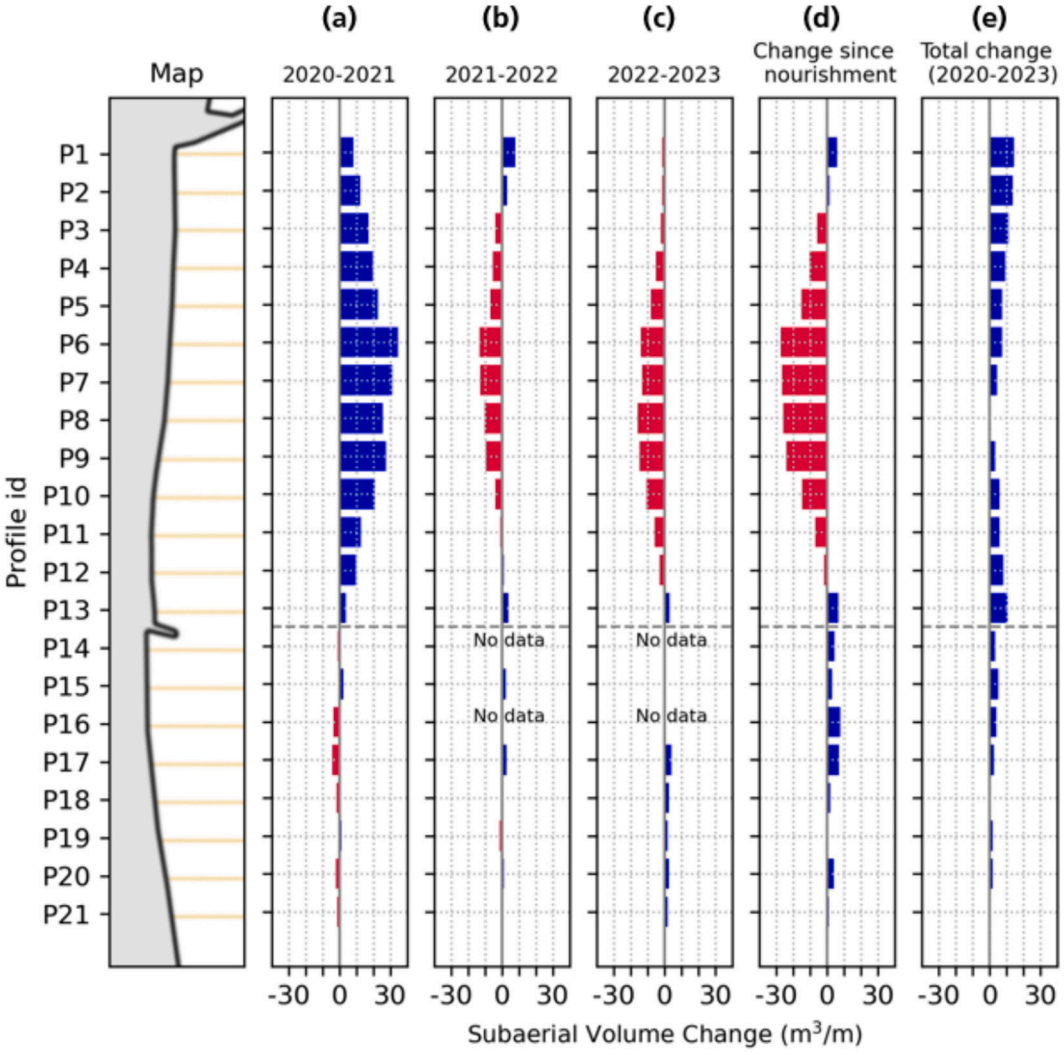


**Fig. 8.** Subaerial volume changes presented for each survey transect and analyzed for a period of three years. The bars align with the location of the survey transects (see the map in the left panel), red indicates erosion and blue indicates deposition.

development of the nourishment. Transects adjacent to the harbor mole (P1, P2) and the groin (P13) are more stable. Furthermore, the subaerial volume in the nourished section is eroding while the downdrift area is increasing in volume over time. Likely, the downdrift area (P14–21) is being supplied with sediment from the nourishment through dominating longshore transport towards the south.

#### 4.2.3. Response under an extreme storm event

The extreme Baltic Sea storm surge 20–21 October 2023 (Babet) affected the nourished stretch and adjacent coastlines at Faxe Ladeplads. It was an eastern storm that generated large waves over the maximum fetch length to reach the site. The conditions before the storm had been dominated by several westerly low pressures that caused elevated water levels in the Baltic Sea basin even before the storm hit. Consequently, the pre-storm profiles measured on 18$^{th}$ October are short because the water level was already elevated to +60 cm DVR90. During the storm, the water levels rose even further due to the strong winds and resulting substantial wind setup and large waves (Fig. 5). The period between 15$^{th}$ June and 18$^{th}$ October 2023 was calm in terms of wave energy (see Fig. 4), which is also reflected in the profile comparisons, with limited change observed for the subaerial beach (see Fig. 9). Hence, profile data from 15$^{th}$ June are considered in the analysis as pre-storm profiles to estimate the elevation change during the storm event since these extend further seawards than the transects from 18$^{th}$ October.

The pre- and post-storm profiles show that the morphological response to the storm varies spatially, illustrated in Fig. 9. Transects P1, P7, P9 and P11 are presented as these are representative for responses observed at different sections along the nourished stretch. Transect P1, close to the harbor mole, shows the least reduction of the beach elevation, and sediment deposition increased the subaerial beach width by 13.5 m in the seaward direction (Fig. 9a). A similar response was observed for P13 which is located by the groin. At the center section of the nourishment, exemplified by transect P7 and P9, scouring occurred at the toe of the revetment (Fig. 9b and c), resulting in the formation of a 0.6 m deep and 10 m wide trench. Generally, the profiles in the mid-part of the nourished section had limited sand volumes in the subaerial part of the beach before the storm (Fig. 9b and c), similar to the pre-nourishment conditions, this part of the beach experienced the most erosion, with elevation change of more than −1 m at the subaerial beach. The eroded material was deposited in a shallow storm bar above mean sea level. The width and elevation of the bar gradually decrease from transect P3 until P10 and the feature becomes less pronounced until it is completely washed out for the section represented by transect P11 (Fig. 9d). Transect P11 displays erosion adjacent to the revetment and material deposition further offshore causing elevation of the subaqueous profile however no bar formation as for the other transects. This spatial variability is also visible in Fig. 10 that shows the opening in the storm bar, possibly washed out by undertow currents over a larger area during high water levels.

The nourishment material from the subaerial beach is eroded and deposited in a storm bar, formed at the lower beach during high water level, that is irregular in the longshore direction, Fig. 10a. There is a substantial erosion and lowering of the subaerial beach, both in the nourished and downdrift area. The nourished section lost 4000 m$^3$ from the subaerial beach (i.e., average 6.15 m$^3$/m) and the downdrift area lost 1750 m$^3$ (i.e., average 4.38 m$^3$/m). When the nourished sand was eroded from the subaerial beach, an underlaying gravel layer was exposed and seaweed was deposited on top (Fig. 10b and c). The pre-storm sediment volume in the subaerial beach shows great variability both for the nourished and downdrift sections. The maximum volume in the nourished area before the storm was found in P1 with 28.84 m$^3$/m. The maximum volume downdrift in P14 with 18.01 m$^3$/m. These

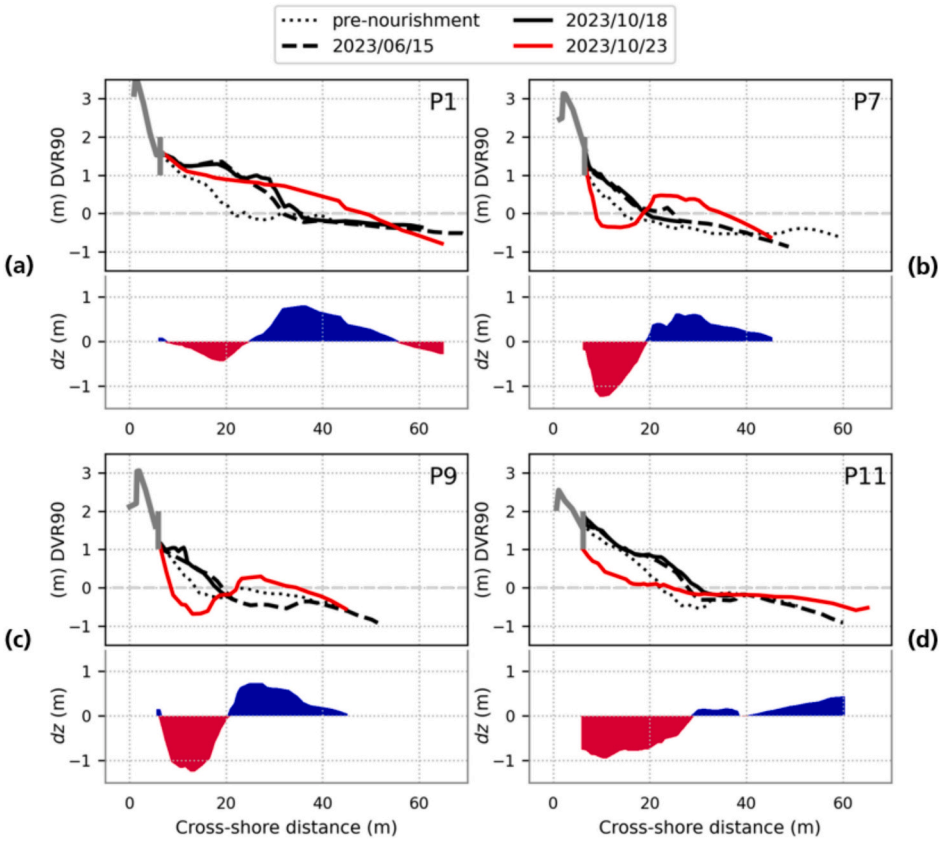


**Fig. 9.** Pre- and post-storm profiles and elevation change for transects P1, P7, P9 and P11. The dotted line corresponds to the 2020/06/09 survey and represents pre-nourishment conditions. Bed level change is computed as the difference between 2023/06/15 and 2023/10/23 surveys, where red indicates erosion and blue indicates deposition.


**Fig. 10.** Images showing the post-storm view of the nourished coastal stretch; (a) drone image from 2023/10/23, Photo: Gregor Luetzenburg (b) before the storm on 2023/10/18, water level is +60 cm, and (c) after the storm on 2023/10/23, water level is +30 cm. The star in (a) indicates the location where pictures (b) and (c) are taken Photo: Anna Adell.

transects are both located at the lee side of shore perpendicular hard structures. The minimum volume in the nourished area before the storm was found in P8 with 5.08 $m^3$/m and the minimum volume downdrift in P18 with 7.26 $m^3$/m. During the storm, a part of the concrete wall behind the rock revetment failed. The impacted distance was approximately 110 m and located landwards from transects P7–9, which had the least subaerial volume before the storm (Fig. 8e).

## 5. Discussion

### 5.1. Initial adjustments after the nourishment

The initial volumetric changes after the placement of the nourishment show that a large reduction in subaerial volume is observed just after an event with relatively high water levels and large waves. This indicates that the morphological response at the site is event-driven. The nourished sediment was eroded, transported from the subaerial beach, and deposited in the nearshore. Material can then be moved onshore and allow for natural recovery and development of sandy features in the profile is possible, which has been observed within the survey period. Observations from other nourishment studies also indicate that the volumetric adjustment can be slow, but the development of morphodynamical features typical for sandy coastlines establishes almost instantly after the deployment (e.g., Brand et al., 2022; Kroon et al., 1995). The current analysis mainly focuses on the subaerial changes as the accuracy of the nearshore single beam measurements is not precise enough to quantify changes further to the depth of closure.

Cross-shore profile adjustment can be a common contributor to rapid losses of nourishment material and have been documented for nourishment actions in sheltered coastal environments (Andrade et al., 2006; Karasu et al., 2023; Ton et al., 2021). At the same time, storm events can speed up the development of nourished coastlines. Elko and Wang (2007) concluded that one single hurricane had the capacity to bring the recently nourished profile to an almost complete equilibrium state. Andrade et al., 2006 observed sediment losses greater than expected in the initial phase due to adjustment towards equilibrium of the foreshore and nearshore slopes at an estuarine pocket beach with meso-tidal conditions. The initial state was characterized by sediment losses due to slope re-adjustment towards the equilibrium and down to the depth of closure.

For the investigated site, storms were identified to play a considerable role in the initial profile adjustment, and substantial erosion was observed in the first months since the nourishment action can be attributed to specific occasions with large waves in combination with high water levels. While limited to no change was observed in low-energy periods. This strongly points to the impact of the episodic energy conditions on the morphological development at the study site. No substantial recovery is observed at the nourished site; the only positive volume change in the dry subaerial beach was observed near the two shore perpendicular structures. The potential for recovery of beaches in low-energy environments is restricted by limited forcing input in the relaxation periods between storms (Gallop et al., 2020) or lack of sediment supply (Kennedy et al., 2023). Adjustments in deeper parts of the profile occur on longer time scales as material in the deep platforms is only activated very occasionally during extreme conditions (Harley et al., 2022; Ton et al., 2021).

### 5.2. Long-term changes over a three-year period

Analysis of the long-term morphological development of the nourished stretch highlights that there is a large spatial variability in the redistribution of sediment and observed volumetric changes. The center section of the nourishment is the most dynamic, while transects located in proximity to the hard structures are more static. Here, beach width and subaerial volume increase over time due to the blocking of longshore drift and is expected to continue until the detainment capacity of the groin is reached. When sediment has accumulated in the edges of the nourished stretch there are no processes that can mobilize the material again. The center section of the nourishment is eroded by both cross-shore processes during storms and longshore processes. The latter

typically transports material in the dominant longshore drift direction southwest or towards the harbor to the northeast depending on the direction of incoming waves. In addition, there is a variability in the underlying bathymetry (Fig. 11) where the 3-m contour line is located more offshore for the northern section (P1-P6) compared to the central section (P7-P13). This creates a more gentle slope for the platform from 3 to 2 m enabling more wave dissipation. This shape likely stems from the location of the harbor, which has a sheltering effect for wave action, which strongly reduces sediment transport capacity. The irregularity in the shoreface bathymetry gives a larger potential for the focus of wave energy to the center section, leading to a strong alongshore variability in the profiles' evolution.

The long-term analysis indicates that the central section (transects P7–9) has lost the subaerial nourishment volume and is back to near pre-nourishment profile configuration after just over two years. Although the nourishment volumes have been distributed from the subaerial beach to adjacent areas and offshore, the protective capabilities are reduced with the reduction of beach width. In a conservative view, this would mean that the lifetime of the 20,000 $m^3$ nourishment is about two years, although largely dependent on intra-annual variation in wave energy and the occurrence of high-magnitude events. The nourishment design with a uniform beach width does not align with the coastline's equilibrium shape, which is suspected to shorten the lifetime. However, the results also show that nourishment material is being transported with the longshore drift and is supplying adjacent coastlines, which is seen as a positive effect over time and a downdrift increase of nearshore volume. In addition, intra-annual and inter-annual variations in wave energy become important for the lifespan of nourishments and are hence a vital part of the understanding for coastal managers (Basterretxea et al., 2007). This makes the estimation of lifetime of soft coastal protection measures difficult.

The presence of the rock revetment limits the landward retreat of the subaerial beach and profiles cannot fully adjust to the wave forcing. In addition, the rock revetment and the road are restricting the beach to adjust to a planar equilibrium shape between the shore-perpendicular structures. The fixed, slightly convex coastline can induce additional gradients in sediment transport, making the center section more vulnerable to erosion. As the beach width is reduced along the nourished coastal stretch, the risk of exposing the rock revetment increases with time as no new sediment is deposited in the center section with natural processes. When the rock revetment is permanently or occasionally exposed during high water level events, there is a risk of increased erosion due to reflective waves on the hard structure (e.g., Bernatchez and Fraser, 2012; Griggs and Tait, 1989).


**Fig. 11.** Map showing the location of 2-, 3-, and 4-m depth contour lines. White points are bathymetry observations from filtered single-beam data, and the lines correspond to the depth contours obtained by fitting a spline function through the points. Background map: Contains data from the Danish Agency for Data Supply and Infrastructure, Ortophoto 2021 geo-denmark_2021_12_5cm, WMS.

### 5.3. Response under an extreme storm event

The extreme storm surge of 20–21 October 2023 represents exceptional surge levels for the region. The rare preconditions for the storm development resembled the conditions during the 1872 Baltic Sea storm surge, when water levels reached above 2.5 m in Faxe Bay (Clemmensen et al., 2014). The observed morphological response of the nourishment and downdrift area was characterized by lowering of the beach elevation, scouring at the toe of the rock revetment, and deposition of nourishment material in a storm bar. Results however clearly show a large spatial variability in physical processes and beach volume change, likely induced by the presence of hard structures. Additionally, the response can possibly be explained by variation in nearshore wave energy dissipation due to variability in the underlying bathymetry previously discussed in section 5.2. Gradients in shoreface bathymetry can be a contributing factor to observed spatial differences in the storm response (Backstrom et al., 2008; Biausque et al., 2022). The observations of storm response at the site are consistent with storm response of beaches with the presence of seawalls or other hard structures (Barnett and Wang, 1989; Jackson and Nordstrom, 1994; Kraus, 1988). In addition, there were differences in the amount of available sand volume in the pre-storm profiles along the investigated coastal stretch. Transects P1 and P14 had more sediment available before the storm and experienced the highest offshore migration of the shoreline due to sediment accumulation on the lee of hard shore-perpendicular structures.

### 5.4. Management implications

Our findings that the morphological response of the nourishment at the site is event driven is consistent with the assessment of the 2018 nourishment (Danish Coastal Authority, 2021), where the authors identified rapid adjustment towards profile equilibrium following specific energetic events. Small-volume interventions can be applied to compensate for seasonal losses. However, simply feeding the stretch with the equivalent volumes to compensate for annual erosion is not enough, as the profile must re-equilibrate (Corradi et al., 2008). For the investigated site, a potential management strategy could be to introduce a bypassing scheme to move material from the updrift side of the harbor to the downdrift side, or to use dredged material from the navigation channel more efficiently. This could be a practical solution to compensate for annual losses or restore the beach after storm impact. It is desired to maintain the beach width in front of the revetment to assure the protective capabilities and positive effect of the nourishment solution.

## 6. Conclusions

This study explores the morphodynamics of a beach nourishment in a partly sheltered embayment in the semi-enclosed Baltic Sea. The energy conditions at the site are highly episodic, which impacts morphological evolution, and observations indicate that the development is event driven. Volumetric recovery is not possible as the energy input in the relaxation periods is limited, and only minor adjustments occur as the establishment of morphological features, such as a beach berm. There is a large spatial variability in the observed change along the nourished stretch where the center section is most susceptible to erosion, and there are edge effects adjacent to hard shore perpendicular structures.

The evolution of the nourishment is characterized by cross-shore transport during storms, altered with periods of longshore processes. The coastal section located downdrift the nourishment is receiving sediment and shows an increase in subaerial volume and widening of the beach and nearshore over time. The lifetime of the nourishment is

estimated to be approximately two years, when a reduction of the subaerial volume and beach width for the most vulnerable transects bring them to near pre-nourishment profile configuration and thereby lower the protective capabilities. However, lifetime is difficult to accurately assess as notable positive effects on adjacent sections are observed, indicating that nourishment material remains in the system. Field observations, remote sensing techniques and monitoring of development are essential datasets for improving design and maintenance strategies for sustainable and resilient coastal protection.

## CRediT authorship contribution statement

**Anna Adell:** Writing – review & editing, Writing – original draft, Visualization, Methodology, Investigation, Formal analysis, Conceptualization. **Aart Kroon:** Writing – review & editing, Supervision, Investigation, Conceptualization. **Björn Almström:** Writing – review & editing, Supervision, Investigation. **Magnus Larson:** Writing – review & editing, Supervision. **Caroline Hallin:** Writing – review & editing, Supervision, Investigation, Funding acquisition.

## Declaration of competing interest

The authors declare that they have no known competing financial interests or personal relationships that could have appeared to influence the work reported in this paper.

## Data availability

Data will be made available on request.

## Acknowledgments

This study was financed by the Swedish Transport Administration (grant number TRV 2019/96299). The authors would like to thank colleagues Paul Christiansen and Drude Fritzbøger Christensen at the University of Copenhagen and Gregor Luetzenburg at the Geological Survey of Denmark and Greenland for valuable support and assistance in the field. Thanks also to Poul Jensen at Faxe Municipality, Klaus Rønholt at Faxe Kalk A/S (Lhoist), and Per Sørensen at the Danish Coastal Authority for help with logistics, data, and local support.

## References

Aagaard, T., 1990. Infragravity waves and nearshore bars in protected, storm-dominated coastal environments. Mar. Geol. 94 (3), 181–203. https://doi.org/10.1016/0025-3227(90)90069-V.

Adell, A., Almström, B., Kroon, A., Larson, M., Uvo, C.B., Hallin, C., 2023. Spatial and temporal wave climate variability along the south coast of Sweden during 1959–2021. Reg. Stud. Mar. Sci. 63, 103011 https://doi.org/10.1016/j.rsma.2023.103011.

Andrade, C., Lira, F., Pereira, M.T., Ramos, R., Guerreiro, J., Freitas, M.C., 2006. Monitoring the nourishment of Santo Amaro Estuarine Beach (Portugal). J. Coast. Res. 776–782. SI 39 (Procredings of the 8th International Coastal Symposium).

Backstrom, J.T., Jackson, D.W.T., Cooper, J.A.G., Malvárez, G.C., 2008. Storm-driven shoreface morphodynamics on a low-wave energy delta: the role of nearshore topography and shoreline orientation. J. Coast. Res. 24 (6), 1379–1387. https://doi.org/10.2112/07-0926.1.

Barbier, E.B., Hacker, S.D., Kennedy, C., Koch, E.W., Stier, A.C., Silliman, B.R., 2011. The value of estuarine and coastal ecosystem services. Ecol. Monogr. 81 (2), 169–193. https://doi.org/10.1890/10-1510.1.

Barnett, M.R., Wang, H., 1989. Effects of a vertical seawall on profile response. In: Proceedings of the 21st Coastal Engineering Conference, pp. 1493–1507.

Basterretxea, G., Orfila, A., Jordi, A., Fornós, J.J., Tintoré, J., 2007. Evaluation of a small volume renourishment strategy on a narrow Mediterranean beach. Geomorphology 88 (1–2), 139–151. https://doi.org/10.1016/j.geomorph.2006.10.019.

Bendixen, M., Clemmensen, L.B., Kroon, A., 2013. Sandy berm and beach-ridge formation in relation to extreme sea-levels: a Danish example in a micro-tidal environment. Mar. Geol. 344, 53–64. https://doi.org/10.1016/j.margeo.2013.07.006.

Beniston, M., Stephenson, D.B., Christensen, O.B., Ferro, C.A.T., Frei, C., Goyette, S., Halsnaes, K., Holt, T., Jylhä, K., Koffi, B., Palutikof, J., Schöll, R., Semmler, T., Woth, K., 2007. Future extreme events in European climate: an exploration of regional climate model projections. Clim. Chang. 81 (Suppl. 1), 71–95. https://doi.org/10.1007/s10584-006-9226-z.

Bernatchez, P., Fraser, C., 2012. Evolution of coastal defence structures and consequences for beach width trends, Québec, Canada. J. Coast. Res. 28 (6), 1550–1566. https://doi.org/10.2112/JCOASTRES-D-10-00189.1.

Biausque, M., Guisado-Pintado, E., Grottoli, E., Jackson, D.W.T., Cooper, J.A.G., 2022. Seasonal morphodynamics of multiple intertidal bars (MITBs) on a meso- to macrotidal beach. Earth Surf. Process. Landf. 47 (3), 839–853. https://doi.org/10.1002/esp.5288.

Blott, S.J., Pye, K., 2004. Morphological and sedimentological changes on an artificially nourished beach, Lincolnshire, UK. J. Coast. Res. 20 (1), 214–233. https://doi.org/10.2112/1551-5036(2004)20[214:mascoa]2.0.co;2.

Booij, N., Ris, R.C., Holthuijsen, L.H., 1999. A third-generation wave model for coastal regions 1. Model description and validation. J. Geophys. Res. Oceans 104 (C4), 7649–7666. https://doi.org/10.1029/98JC02622.

Brand, E., Ramaekers, G., Lodder, Q., 2022. Dutch experience with sand nourishments for dynamic coastline conservation – an operational overview. Ocean Coast. Manag. 217, 106008 https://doi.org/10.1016/j.ocecoaman.2021.106008.

Clemmensen, L.B., Bendixen, M., Hede, M.U., Kroon, A., Nielsen, L., Murray, A.S., 2014. Morphological records of storm floods exemplified by the impact of the 1872 Baltic storm on a sandy spit system in south-eastern Denmark. Earth Surf. Process. Landf. 39 (4), 499–508. https://doi.org/10.1002/esp.3466.

Corradi, N., Ferrari, M., Schiaffino, C.F., 2008. Evaluation of the effectiveness of a seasonal nourishment programme of the pocket beaches of the city of Genoa. Chem. Ecol. 24 (1), 215–223. https://doi.org/10.1080/02757540801965472.

Danish Coastal Authority, 2021. Beach Nourishment Effects - Faxe Ladeplads.

Davidson-Arnott, R., 2010. Introduction to Coastal Processes and Geomorphology. Cambridge University Press.

De Schipper, M.A., De Vries, S., Ruessink, G., De Zeeuw, R.C., Rutten, J., Van Gelder-Maas, C., Stive, M.J.F., 2016. Initial spreading of a mega feeder nourishment: Observations of the Sand Engine pilot project. Coast. Eng. 111, 23–38. https://doi.org/10.1016/j.coastaleng.2015.10.011.

De Schipper, M.A., Ludka, B.C., Raubenheimer, B., Luijendijk, A.P., Schlacher, T.A., 2021. Beach nourishment has complex implications for the future of sandy shores. Nature Reviews Earth and Environment 2 (1), 70–84. https://doi.org/10.1038/s43017-020-00109-9.

Dean, R.G., 2002. Beach Nourishment: Theory and Practice. World Scientific Publishing.

Defeo, O., McLachlan, A., Schoeman, D.S., Schlacher, T.A., Dugan, J., Jones, A., Lastra, M., Scapini, F., 2009. Threats to sandy beach ecosystems: a review. Estuar. Coast. Shelf Sci. 81 (1), 1–12. https://doi.org/10.1016/j.ecss.2008.09.022.

Dissanayake, P., Winter, C., Averes, T., Krämer, K., Sone, H., Dreier, N., Nehlsen, E., Fröhle, P., Hirschhäuser, T., 2023. Effect of large-scale forcing on the local sediment transport potential at the Schleswig-Holstein Baltic Sea Coast. Coastal Engineering Proceedings 37, 5. https://doi.org/10.9753/icce.v37.sediment.5.

Eelsalu, M., Parnell, K.E., Soomere, T., 2022. Sandy beach evolution in the low-energy microtidal Baltic Sea: attribution of changes to hydrometerological forcing. Geomorphology 414 (July), 108383. https://doi.org/10.1016/j.geomorph.2022.108383.

Elko, N.A., Wang, P., 2007. Immediate profile and planform evolution of a beach nourishment project with hurricane influences. Coast. Eng. 54 (1), 49–66. https://doi.org/10.1016/j.coastaleng.2006.08.001.

Gallop, S.L., Vila-Concejo, A., Fellowes, T.E., Harley, M.D., Rahbani, M., Largier, J.L., 2020. Wave direction shift triggered severe erosion of beaches in estuaries and bays with limited post-storm recovery. Earth Surf. Process. Landf. 45 (15), 3854–3868. https://doi.org/10.1002/esp.5005.

Griggs, G.B., Tait, J.F., 1989. Observations of the end effects of seawalls. Shore and Beach 57, 25–26.

Hallin, C., Hofstede, J.L.A., Martinez, G., Jensen, J., Baron, N., Heimann, T., Kroon, A., Arns, A., Almström, B., Sørensen, P., Larson, M., 2021. A comparative study of the effects of the 1872 storm and coastal flood risk management in Denmark, Germany, and Sweden. Water (Switzerland) 13 (12), 1–22. https://doi.org/10.3390/w13121697.

Hanson, H., Larson, M., 2008. Implications of extreme waves and water levels in the southern Baltic Sea. J. Hydraul. Res. 46 (2), 292–302. https://doi.org/10.1080/00221686.2008.9521962.

Hanson, H., Brampton, A., Capobianco, M., Dette, H.H., Hamm, L., Laustrup, C., Lechuga, A., Spanhoff, R., 2002. Beach nourishment projects, practices, and objectives - a European overview. Coast. Eng. 47 (2), 81–111. https://doi.org/10.1016/S0378-3839(02)00122-9.

Harff, J., Deng, J., Dudzińska-Nowak, J., Fröhle, P., Groh, A., Hünicke, B., Soomere, T., Zhang, W., 2017. What determines the change of coastlines in the Baltic Sea? In: Harff, J., Furmanczyk, K., VonStorch, H. (Eds.), Coastline Changes of the Baltic Sea from South to East. Springer International Publishing. https://doi.org/10.1007/978-3-319-49894-2_6.

Harley, M.D., Masselink, G., Ruiz de Alegría-Arzaburu, A., Valiente, N.G., Scott, T., 2022. Single extreme storm sequence can offset decades of shoreline retreat projected to result from sea-level rise. Communications Earth and Environment 3 (1), 1–11. https://doi.org/10.1038/s43247-022-00437-2.

Hellström, B., 1941. Vattenståndsvariationerna i Östersjöbäckenet. In: Väg- och Vattenbyggnadskonst Husbyggnadsteknik.

Hünicke, B., Zorita, E., Soomere, T., Madsen, K.S., Johansson, M., Suursaar, Ü., 2015. Recent Change—Sea Level and Wind Waves. https://doi.org/10.1007/978-3-319-16006-1_9.

Jackson, N.L., Nordstrom, K.F., 1994. The mobility of beach fill in front of a seawall on an estuarine shoreline, Cliffwood Beach, New Jersey, USA. Ocean Coast. Manag. 23 (2), 149–166. https://doi.org/10.1016/0964-5691(94)90062-0.

Jackson, N.L., Nordstrom, K.F., Eliot, I., Masselink, G., 2002. "Low energy" sandy beaches in marine and estuarine environments a review. Geomorphology 48 (1–3), 147–162. https://doi.org/10.1016/S0169-555X(02)00179-4.

Johansson, M., Boman, H., Kahma, K.K., Launiainen, J., 2001. Trends in sea level variability in the Baltic Sea. Boreal Environ. Res. 6 (3), 159–179.

Karasu, S., Marangoz, H.O., Gülkaya, E., Akpınar, A., Ceylan, Y., Yılmaz, E., 2023. Performance based assessment of a small-scale artificially nourished beach. Ocean Coast. Manag. 244 (August) https://doi.org/10.1016/j.ocecoaman.2023.106827.

Kennedy, D.M., McCarroll, R.J., Fellowes, T.E., Gallop, S.L., Pucino, N., McSweeney, S.L., Vila-Concejo, A., Reef, R., Yuan, R., Carvalho, R., Quang, T.H., Ierodiaconou, D., 2023. Drivers of seasonal and decadal change on an estuarine beach in a fetch-limited temperate embayment. Mar. Geol. 463 (June), 107130 https://doi.org/10.1016/j.margeo.2023.107130.

Kraus, N.C., 1988. Effects of seawalls on the beach: a literature review. J. Coast. Res. SI (4),, 1–28.

Kroon, Aart, Hoekstra, P., Houwman, K., Ruessink, G., 1995. Morphological monitoring of shoreface nourishment Nourtech - Experiment at Terschelling, The Netherlands. In: Edge, B.L. (Ed.), Coastal Engineering 1994: Proceedings of the Twenty-Fourth International Conference, pp. 2222–2236.

Kroon, Anna, De Schipper, M., De Vries, S., Aarninkhof, S., 2022. Subaqueous and subaerial beach changes after implementation of a mega nourishment in front of a sea dike. Journal of Marine Science and Engineering 10 (8). https://doi.org/10.3390/jmse10081152.

Leppäranta, M., Myrberg, K., 2009. Physical oceanography of the Baltic Sea. In: Paper Knowledge. Toward a Media History of Documents.

Lowe, M.K., Kennedy, D.M., 2016. Stability of artificial beaches in port Phillip Bay, Victoria, Australia. J. Coast. Res. 1 (75), 253–257. https://doi.org/10.2112/SI75-51.1.

Luetzenburg, G., Bjørk, A.A., Svennevig, K., Kroon, A., 2023. Drivers of coastal cliff erosion in Denmark. Coastal Sediments 2023, 1272–1285. https://doi.org/10.1142/9789811275135_0118.

Luijendijk, A., Hagenaars, G., Ranasinghe, R., Baart, F., Donchyts, G., Aarninkhof, S., 2018. The state of the world's beaches. Sci. Rep. 8 (1), 1–11. https://doi.org/10.1038/s41598-018-24630-6.

Masetti, G., Andersen, O., Andreasen, N.R., Christiansen, P.S., Cole, M.A., Harris, J.P., Langdahl, K., Schwenger, L.M., Sonne, I.B., 2022. Denmark's depth model: compilation of bathymetric data within the Danish waters. Geomatics 2 (4), 486–498. https://doi.org/10.3390/geomatics2040026.

Metzner, M., Gade, M., Hennings, I., Rabinovich, A.B., 2000. The observation of seiches in the Baltic Sea using a multi data set of water levels. J. Mar. Syst. 24 (1–2), 67–84. https://doi.org/10.1016/S0924-7963(99)00079-2.

Muñoz-Perez, J.J., De San, Lopez, Roman-Blanco, B., Gutierrez-Mas, J.M., Moreno, L., Cuena, G.J., 2001. Cost of beach maintenance in the Gulf of Cadiz (SW Spain). Coast. Eng. 42 (2), 143–153. https://doi.org/10.1016/S0378-3839(00)00054-5.

Nielsen, P., 2009. Coastal and Estuarine Processes. World Scientific Publishing.

O'Brien, M.K., Valverde, H.R., Trembanis, A.C., Haddad, T.C., 1999. Summary of beach nourishment activity along the Great Lakes' shoreline 1955-1996. J. Coast. Res. 15 (1), 206–219.

Ojeda, E., Guillén, J., 2008. Shoreline dynamics and beach rotation of artificial embayed beaches. Mar. Geol. 253 (1–2), 51–62. https://doi.org/10.1016/j.margeo.2008.03.010.

Omstedt, A., Pettersen, C., Rodhe, J., Winsor, P., 2004. Baltic Sea climate: 200 yr of data on air temperature, sea level variation, ice cover, and atmospheric circulation. Clim. Res. 25 (3), 205–216. https://doi.org/10.3354/cr025205.

Oppenheimer, M., Glavovic, B.C., Hinkel, J., van de Wal, R., Magnan, A.K., Abd-Elgawad, A., Cai, R., Cifuentes-Jara, M., DeConto, R.M., Ghosh, T., Hay, J., Isla, F., Marzeion, B., Meyssignac, B., Sebesvari, Z., 2019. Sea level rise and implications for low-lying islands, coasts and communities coordinating. In: Pörtner, H.-O., Roberts, D.C., Masson-Delmotte, V., Zhai, P., Tignor, M., Poloczanska, E., Mintenbeck, K., Alegría, A., Nicolai, M., Okem, A., Petzold, J., Rama, B. (Eds.), N. M. W. IPCC Special Report on the Ocean and Cryosphere in a Changing Climate.

Orvikut, K., Jaagus, J., Kont, A., Ratas, U., Rivis, R., 2003. Increasing activity of coastal processes associated with climate change in Estonia. J. Coast. Res. 19 (2), 364–375.

Pilkey, O.H., Clayton, T.D., Journal, S., Winter, N., Pilkey, O.H., Clayton, T.D., 1989. Summary of beach replenishment experience on U. S. east coast barrier islands, 5 (1), 147–159.

Pupienis, D., Jarmalavičius, D., Žilinskas, G., Fedorovič, J., 2014. Beach nourishment experiment in Palanga, Lithuania. J. Coast. Res. 70, 490–495. https://doi.org/10.2112/SI70-083.1.

Spodar, A., Héquette, A., Ruz, M.H., Cartier, A., Grégoire, P., Sipka, V., Forain, N., 2018. Evolution of a beach nourishment project using dredged sand from navigation channel, Dunkirk, northern France. J. Coast. Conserv. 22 (3), 457–474. https://doi.org/10.1007/s11852-017-0514-8.

Stive, M.J.F., De Schipper, M.A., Luijendijk, A.P., Aarninkhof, S.G.J., Van Gelder-Maas, C., Van Thiel De Vries, J.S.M., De Vries, S., Henriquez, M., Marx, S., Ranasinghe, R., 2013. A new alternative to saving our beaches from sea-level rise: the sand engine. J. Coast. Res. 29 (5), 1001–1008. https://doi.org/10.2112/JCOASTRES-D-13-00070.1.

Suursaar, Ü., Jaagus, J., Kullas, T., 2006. Past and future changes in sea level near the Estonian coast in relation to changes in wind climate. Boreal Environ. Res. 11 (2), 123–142.

Swedish Meteorological and Hydrological Institute, 2023. Stormflod under Babet oktober 2023. Kunskapsbanken. https://www.smhi.se/kunskapsbanken/oceanografi/hogvattenhandelser-i-sverige/stormflod-oktober-2023-1.201721.

Ton, A.M., Vuik, V., Aarninkhof, S.G.J., 2021. Sandy beaches in low-energy, non-tidal environments: linking morphological development to hydrodynamic forcing. Geomorphology 374, 107522. https://doi.org/10.1016/j.geomorph.2020.107522.

Van Rijn, L.C., 2011. Coastal erosion and control. Ocean Coast. Manag. 54 (12), 867–887. https://doi.org/10.1016/j.ocecoaman.2011.05.004.

Vos, K., Harley, M.D., Turner, I.L., Splinter, K.D., 2023. Pacific shoreline erosion and accretion patterns controlled by El Niño/Southern Oscillation. Nat. Geosci. 16 (2), 140–146. https://doi.org/10.1038/s41561-022-01117-8.

Vousdoukas, M.I., Mentaschi, L., Voukouvalas, E., Verlaan, M., Feyen, L., 2017. Extreme sea levels on the rise along Europe's coasts. Earth's Future 5 (3), 304–323. https://doi.org/10.1002/2016EF000505.

Vousdoukas, M.I., Ranasinghe, R., Mentaschi, L., Plomaritis, T.A., Athanasiou, P., Luijendijk, A., Feyen, L., 2020. Sandy coastlines under threat of erosion. Nat. Clim. Chang. 10 (3), 260–263. https://doi.org/10.1038/s41558-020-0697-0.

Weisse, R., Dailidiene, I., Hünicke, B., Kahma, K., Madsen, K., Omstedt, A., Parnell, K., Schöne, T., Soomere, T., Zhang, W., Zorita, E., 2021. Sea level dynamics and coastal erosion in the Baltic Sea region. Earth Syst. Dynam. 12 (3), 871–898. https://doi.org/10.5194/esd-12-871-2021.

Woolf, D.K., Shaw, A.G.P., Tsimplis, M.N., 2003. The influence of the North Atlantic Oscillation on sea-level variability in the North Atlantic region. Global Atmosphere and Ocean System 9 (4), 145–167. https://doi.org/10.1080/10236730310001633803.